

Control of Cellular Physiology by TM9 Proteins in Yeast and *Dictyostelium**

Romain Froquet[‡], Nathalie Cherix[‡], Raphael Birke[§], Mohammed Benghezal[‡], Elisabetta Cameroni[¶], François Letourneur^{||}, Hans-Ulrich Mösch[§], Claudio De Virgilio[¶], and Pierre Cosson^{‡1}

From the [‡]Département de Physiologie et Métabolisme Cellulaire, Centre Médical Universitaire, Université de Genève, rue Michel Servet 1, CH-1211 Genève 4, Switzerland, [§]Department of Genetics, Philipps University Marburg, Karl-von-Frisch-Strasse 8, D-35043 Marburg, Germany, the [¶]Department of Medicine, University of Fribourg, Division of Biochemistry, 1700 Fribourg, Switzerland, and the ^{||}Institut de Biologie et Chimie des Protéines, UMR 5086, CNRS, Université Lyon 1, IFR128 BioSciences Lyon-Gerland, 7, Passage du Vercors, 69367 Lyon Cedex 07, France

TM9 proteins constitute a well defined family, characterized by the presence of a large variable extracellular domain and nine putative transmembrane domains. This family is highly conserved throughout evolution and comprises three members in *Dictyostelium discoideum* and *Saccharomyces cerevisiae* and four in humans and mice. In *Dictyostelium*, previous analysis demonstrated that TM9 proteins are implicated in cellular adhesion. In this study, we generated TM9 mutants in *S. cerevisiae* and analyzed their phenotype with particular attention to cellular adhesion. *S. cerevisiae* strains lacking any one of the three TM9 proteins were severely suppressed for adhesive growth and filamentous growth under conditions of nitrogen starvation. In these mutants, expression of the *FLO11-lacZ* reporter gene was strongly reduced, whereas expression of *FRE(Ty1)-lacZ* was not, suggesting that TM9 proteins are implicated at a late stage of nutrient-controlled signaling pathways. We also reexamined the phenotype of *Dictyostelium* TM9 mutant cells, focusing on nutrient-controlled cellular functions. Although the initiation of multicellular development and autophagy was unaltered in *Dictyostelium* TM9 mutants, nutrient-controlled secretion of lysosomal enzymes was dysregulated in these cells. These results suggest that in both yeast and amoebae, TM9 proteins participate in the control of specific cellular functions in response to changing nutrient conditions.

TM9 proteins constitute a well defined family of proteins characterized by the presence of nine transmembrane domains and a high degree of similarity (1). There are three members of this family in *Saccharomyces cerevisiae*, *Dictyostelium* amoebae, and *Drosophila* flies and four in humans and mice (2). Although their high degree of evolutionary conservation suggests that they play an important role in cellular physiology, little is known about the role of TM9 proteins. The most

detailed studies to date concerning the role of TM9 proteins stem from the study of *Dictyostelium* amoebae.

The cellular slime mold *Dictyostelium discoideum* has been used previously as a model organism to study phagocytosis and the endocytic pathway. During the course of a systematic search for mutants affected in phagocytosis, a mutant cell line with a defective TM9 protein (named Phg1 or Phg1a) was identified (3). Loss of Phg1a function led to a defect in cellular adhesion, resulting in inefficient phagocytosis. Although it was initially proposed that Phg1a might be an adhesion molecule (3), a more detailed analysis suggested that it might rather indirectly affect cell adhesion by controlling the cell surface level of an as yet unidentified cell surface adhesion molecule (2). There are two other members in the TM9 family in *Dictyostelium* (Phg1b and Phg1c) and Phg1a and Phg1b appear to play synergistic roles in the control of cell adhesion (2). In yeast or in human, the function of TM9 proteins has essentially not been studied.

To understand better the function of TM9 proteins, we analyzed the phenotypes of TM9 mutants in *S. cerevisiae* as well as in *D. discoideum*. Our results suggest that TM9 proteins play a role in late stages of a nutrient-controlled signaling cascade that ultimately controls cellular adhesion and filamentous growth in *S. cerevisiae*. Similarly, *D. discoideum* TM9 proteins, in addition to their role in cellular adhesion, appear to be involved in nutrient-controlled steps of intracellular transport.

EXPERIMENTAL PROCEDURES

Cells and Reagents—All of the yeast strains used in this study were obtained in the Σ 1278b genetic background and are described in Table 1. Yeast transformation was performed using the lithium acetate method (4). Each TM9 gene was deleted by PCR-mediated gene disruption, using the G418 resistance gene cassette derived from template plasmid pFA6-kanMX2 (5, 6) or the *HIS3* or *TRP1* gene cassette derived from template plasmids pRS303 and pRS304, respectively. Double and triple TM9 knock-out mutants were obtained by crossing the single knock-out strains. The yeast plasmids used in this study are described in Table 2.

D. discoideum strains were grown in HL5 medium at 21 °C and subcultured twice a week to maintain a maximal density of 10⁶ cells/ml. All of the mutant strains used in this study were derived from the subclone DH1–10 (3) of the axenic *Dictyostelium* strain DH1, previously derived from nonaxenic wild-type

* This work was supported by Fonds National Suisse de la Recherche Scientifique Grants 3100A0-108078 (to P. C.) and PP00A-106754/1 (to C. D. V.). This work was also supported in part by the 3R Foundation. The costs of publication of this article were defrayed in part by the payment of page charges. This article must therefore be hereby marked "advertisement" in accordance with 18 U.S.C. Section 1734 solely to indicate this fact.

¹ To whom correspondence should be addressed. Tel.: 41-22-379-5293; Fax: 41-22-379-5338; E-mail: Pierre.Cosson@medecine.unige.ch.

TABLE 1**Yeast strains used in this study**

Strain	Genotype	Source
YHUM216	<i>MATa ura3-52 leu2 his3</i>	H. U. Mösch lab collection
YHUM217	<i>MATa ura3-52 leu2 his3</i>	H. U. Mösch lab collection
YHUM305	<i>MATa ura3-52 leu2 trp1</i>	H. U. Mösch lab collection
YHUM306	<i>MATa ura3-52 leu2 trp1</i>	H. U. Mösch lab collection
YRF1	<i>MATa ura3-52 leu2 his3 Tmn1Δ::kanMX</i>	This study
YRF10	<i>MATa ura3-52 leu2 his3 Tmn1Δ::kanMX</i>	This study
YRF2	<i>MATa ura3-52 leu2 trp1 tmn2Δ::TRP1</i>	This study
YRF20	<i>MATa ura3-52 leu2 trp1 tmn2Δ::TRP1</i>	This study
YRF3	<i>MATa ura3-52 leu2 his3 tmn3Δ::HIS3</i>	This study
YRF30	<i>MATa ura3-52 leu2 his3 tmn3Δ::HIS3</i>	This study
YRF4	<i>MATa ura3-52 leu2 trp1 Tmn1Δ::kanMX tmn2Δ::TRP1</i>	This study
YRF5	<i>MATa ura3-52 leu2 Tmn1Δ::kanMX tmn3Δ::HIS3</i>	This study
YRF6	<i>MATa ura3-52 leu2 trp1 tmn2Δ::TRP1 tmn3Δ::HIS3</i>	This study
YRF7	<i>MATa ura3-52 leu2 trp1 Tmn1Δ::kanMX tmn2Δ::TRP1 tmn3Δ::HIS3</i>	This study
YRF100	<i>MATa/MATa ura3-52/ura3-52 leu2/leu2 his3/HIS3 TRP1/trp1</i>	This study
YRF11	<i>MATa/MATa ura3-52/ura3-52 leu2/leu2 his3/HIS3 trp1/TRP1 Tmn1Δ::kanMX/Tmn1Δ::kanMX</i>	This study
YRF22	<i>MATa/MATa ura3-52/ura3-52 leu2/leu2 trp1/trp1 tmn2Δ::TRP1/tmn2Δ::TRP1</i>	This study
YRF33	<i>MATa/MATa ura3-52/ura3-52 leu2/leu2 his3/his3 tmn3Δ::HIS3/tmn3Δ::HIS3</i>	This study
YRF44	<i>MATa/MATa ura3-52/ura3-52 leu2/leu2 trp1/trp1 Tmn1Δ::kanMX/Tmn1Δ::kanMX tmn2Δ::TRP1/tmn2Δ::TRP1</i>	This study
YRF55	<i>MATa/MATa ura3-52/ura3-52 leu2/leu2 Tmn1Δ::kanMX/Tmn1Δ::kanMX tmn3Δ::HIS3/tmn3Δ::HIS3</i>	This study
YRF66	<i>MATa/MATa ura3-52/ura3-52 leu2/leu2 trp1/trp1 tmn2Δ::TRP1/tmn2Δ::TRP1 tmn3Δ::HIS3/tmn3Δ::HIS3</i>	This study
YRF77	<i>MATa/MATa ura3-52/ura3-52 leu2/leu2 trp1/trp1 Tmn1Δ::kanMX/Tmn1Δ::kanMX tmn2Δ::TRP1/tmn2Δ::TRP1 tmn3Δ::HIS3/tmn3Δ::HIS3</i>	This study

TABLE 2**Plasmids used in this study**

Plasmid	Description	Reference
pFA6-kanMX2	kan ^r fused to TEF promoter and terminator in pFA6	Ref. 5
pRS303	pBluescript, <i>HIS3</i>	Ref. 41
pRS304	pBluescript, <i>TRP1</i>	Ref. 41
pYEp213-Ras2-Val ¹⁹	pYEp213::RAS2Val ¹⁹ (2μ, LEU2, amp ^r)	Ref. 13
pSEY18-TOR1	pSEY18::TOR1-1 (2μ, URA3, amp ^r)	Ref. 14
pFRE(Ty1)::LacZ	pLG669-Z::FRE(Ty1) (2μ, URA3, amp ^r)	Ref. 17
B3782	3kb FLO11 promoter fragment in YEpl355	Ref. 16

cells (7). For simplicity, DH1–10 cells are referred to as wild-type cells. The *phg1a* (3), *phg1b* (2), *phg1a* overexpressing *Phg1b* (2), the double *phg1a/phg1b* (2), *phg2* (8), and *apm1* (9) mutant strains were described previously. Rabbit polyclonal antibodies to *Dictyostelium* cathepsin D (10) was a kind gift from Dr. J. Garin (CEA, Grenoble, France). The contact site A protein was detected with monoclonal antibodies 33-294-17 (11).

Phylogenetic Tree—The phylogenetic tree of TM9 proteins in *D. discoideum* (*Phg1a*, *b*, *c*), human (TM9SF1, 2, 3, and 4), and *S. cerevisiae* (*Tmn1*, *Tmn2*, and *Tmn3*) was obtained using clustalW software from the European Bioinformatics Institute. The corresponding accession numbers are: TM9SF1-O15321, TM9SF2(p76)-Q99805, TM9SF3 (hSMBP)-Q9HD45, TM9SF4-Q92544, *Phg1a*-Aj318760, *Phg1b*-Aj507828, *Phg1c*-Aj507829, *Tmn1*-S000004073, *Tmn2*-S000002514, and *Tmn3*-S000000915.

Yeast Adhesive and Filamentous Growth—To observe adhesive growth, haploid yeast strains were plated on YPD for 4 days at 30 °C. The plates were photographed before and after washing with distilled water to visualize the remaining adherent cells. To induce filamentous growth, diploid yeast cells were grown on synthetic low ammonia dextrose agar plates for 3 days at 30 °C (12). Pictures of the agar plates were taken with a Zeiss Axiophot 1 equipped with an Axiocam color camera (Carl Zeiss MicroImaging Inc.). When indicated, the dominant active *RAS2*^{Val19} allele was expressed using the YEpl-Ras2^{Val19} plasmid (13). *TOR1* (target of rapamycin 1) was overexpressed using the pSEY18-TOR1 plasmid (14).

β-Galactosidase Assays—Expression of *FLO11-lacZ* and *FRE(Ty1)-lacZ* reporter genes was determined as previously described (15–17) by measuring β-galactosidase activity in haploid or diploid yeast strains transformed with the corresponding plasmids. *FRE(Ty1)-lacZ* plasmid was a kind gift from Dr. H. D. Madhani (UCSF, San Francisco, CA). The cells were grown in liquid YNB medium to exponential growth phase (8 h), washed with breaking buffer (100 mM Tris-HCl, pH 8, 20% glycerine), and pelleted. The cell pellets were resuspended with 250 μl of breaking buffer containing 1 mM dithiothreitol and 5 mM phenylmethylsulfonyl fluoride and lysed mechanically by vortexing samples with glass beads at 4 °C. Cell extracts (10 μl) were added to 200 μl of Z buffer (60 mM Na₂HPO₄, 40 mM NaH₂PO₄, 10 mM KCl, 1 mM MgSO₄, 50 mM mercaptoethanol, pH 7) and incubated for 5 min at 28 °C. Enzymatic activity was revealed with 5 mM 2-nitrophenyl β-D-galactopyranoside and was stopped with 220 mM Na₂CO₃. The activities were normalized to the total protein in each extract using a Bio-Rad protein assay kit. β-Galactosidase specific activity equals ($A_{420} \times 0.304$)/(0.0045 × protein × extract volume × time) (15, 18).

Secretion of Lysosomal Enzymes by Dictyostelium Cells—Secretion of lysosomal enzymes was assessed as described previously (19). Briefly, to measure secretion kinetics, the cells were harvested, washed, and resuspended at 10⁶ cells/ml in fresh HL5 and then incubated at 21 °C with mild shaking. At each indicated time, an aliquot of the cell suspension was recovered and centrifuged. To assess enzymatic activity, 50 μl of sample (supernatants or cell pellets resuspended in 0.1% Triton-X-100) and 50 μl of substrate mix (10 mM substrate in 5 mM NaOAc, pH 5.2) were mixed and incubated for ~1 h at 37 °C. The reaction was stopped with 500 mM Na₂CO₃, and the optical density at 405 nm was determined in a microplate enzyme-linked immunosorbent assay reader.

Enzyme substrates (Sigma) were dissolved in dimethylformamide at a concentration of 250 mM and stored at –20 °C. *p*-Nitrophenyl phosphate, *p*-nitrophenyl *N*-acetyl β-D-glucosamide, and *p*-nitrophenyl-α-D-mannopyranoside were used as sub-

strates for acid phosphatase, *N*-acetyl β -glucosaminidase, and α -mannosidase, respectively.

To examine the constitutive secretion of lysosomal enzymes over longer periods of time, the cells were grown in HL5 medium for 3 days to a final density of 2×10^6 cells/ml, and then enzymatic activities were determined in the cell pellets and in the supernatants as described above.

Multicellular Development of *Dictyostelium Amoebae*—The ability of *Dictyostelium* amoebae to initiate multicellular development was assessed as previously described (20). Briefly, the cells were harvested at a density of 10^6 cells/ml, washed in HL5, and plated at 10^6 cells/ml in Petri dishes containing HL5 diluted with phosphate buffer (2 mM Na_2HPO_4 , 14.7 KH_2PO_4 , pH 6.5) as indicated. The cells were incubated at 21 °C to allow development. The presence of multicellular aggregates and the expression of contact site A (csA)² were assessed after 24 h. Depending on the batch of tryptone used for the preparation of the HL5 medium, the concentration of HL5 needed to inhibit development of wild-type *Dictyostelium* varied significantly (data not shown). This accounts for the fact that the results presented in this study are quantitatively different from results presented in a previous study (20).

Western Blot Analysis—To test whether secreted lysosomal enzymes had undergone proteolytic maturation in endosomal compartments, the cells were incubated in HL5 medium for 3 days. 10^6 cells were harvested and centrifuged. Proteins in supernatants were precipitated with trichloroacetic acid. Cellular pellets and precipitated supernatants were resuspended in sample buffer (0.103 g/ml sucrose, 5×10^{-2} M Tris, pH 6.8, 5×10^{-3} M EDTA, 0.5 mg/ml bromophenol blue, 2% SDS), and proteins were separated on a 10% polyacrylamide gel and transferred onto a nitrocellulose Protran BA 85 membrane (Schleicher & Schuell). The membranes were incubated with an anti-cathepsin D rabbit antiserum (1/1500) and then with a horseradish peroxidase-coupled goat anti-rabbit IgG (Bio-Rad), washed, and revealed by enhanced chemiluminescence (Amersham Biosciences).

To assess csA expression, 1.5×10^6 cells were harvested and lysed in 40 μl of sample buffer. Proteins (15 μl) were separated on a 10% polyacrylamide gel in reducing conditions and transferred onto nitrocellulose. The membranes were incubated with the anti-csA antibody and then with a horseradish peroxidase-coupled donkey anti-mouse immunoglobulin (Amersham Biosciences), washed, and revealed by enhanced chemiluminescence.

Real Time PCR—The cells (wild-type cells, *phg2* cells, and all the *phg1* mutants) were grown in HL5 medium for 3 days to a final density of 10^6 cells/ml. As a positive control, 10^7 of each mutant cells were incubated for 6 h in phosphate buffer to allow induction of autophagy genes. The cells were harvested, and RNAs were purified with a NucleoSpin RNA II kit (Macherey-Nagel, Duren, Germany). The Agilent 2100 Bioanalyzer (Agilent Technologies, Santa Clara, CA) was used to assess RNA quality. cDNA was synthesized from 1 μg of total RNA using random hexamers and Superscript II reverse transcriptase

(Invitrogen). Amplicons were designed over exon boundaries using the program Primer Express v 2.0 (Applied Biosystems, Foster City, CA) with default parameters. The sequences were aligned against the *Dictyostelium* genome by BLAST to ensure that they were specific for the gene being tested. Oligonucleotides were obtained from Invitrogen, and the sequences are as follows: ATG1, 5'-aaacaaatgaaccctttgccata-3' and 5'-ccgcta-atctacaacatcgacaac-3'; ATG8, 5'-aacgaccaccactcgacaa-3' and 5'-tgatctaatacgttcagctactctcttc-3'; and ATG9, 5'-ttaaact-ggaagagtcgacaaa-3' and 5'-ggagatcgttgacagcgtttaaa-3'. The efficiency of each design was tested with serial dilutions of cDNA. PCRs (10 μl volume) contained diluted cDNA (16 ng), SYBR Green Master Mix (Applied Biosystems), and 300 nM of forward and reverse primers. PCR was performed on a SDS 7900 HT instrument (Applied Biosystems) with the following parameters: 50 °C for 2 min, 95 °C for 10 min, and 40 cycles of 95 °C 15 s to 60 °C 1 min. Each reaction was performed in triplicate on 384-well plates. Raw C_t values obtained with SDS 2.2.2 (Applied Biosystems) were imported in Excel (Microsoft Corporation) and normalization factors, and fold changes were calculated.

Fluid Phase Uptake and Recycling—To measure fluid phase uptake, the cells were incubated for 1 h in HL5 containing 10 $\mu\text{g}/\text{ml}$ of Alexa 647-coupled dextran (Molecular Probes, Oregon, WA) at 21 °C. The cells were then washed, and internalized fluorescence was measured. To analyze recycling, the cells were pulsed with HL5 containing 10 $\mu\text{g}/\text{ml}$ of Alexa 647-coupled dextran for 2 h. The cells were then chased for various times by incubation in HL5 medium at 21 °C without dextran. The remaining internal fluorescence was measured by flow cytometry using a Becton Dickinson FACSCalibur (San Jose, CA).

RESULTS

TM9 Proteins in *S. cerevisiae*—Three genes encoding members of the TM9 family can be identified in the budding yeast *S. cerevisiae* genome: YLR083c (*TMN1* (transmembrane 1)), YDR107c (*TMN2*), and YER113c (*TMN3*). Tmn1 (also called Emp70) was previously described as an endosomal membrane protein (21), and it is 86 and 41% similar to Tmn2 and Tmn3 proteins, respectively. As described earlier (2, 22), TM9 proteins can be separated in two groups. Group I is characterized by a conserved motif at position 50 (VGPYXNXQETY) and a short N-terminal domain (220 amino acids), whereas group II exhibits a characteristic sequence immediately after the signal peptide (FY(V/L)PG(VL)AP), and a longer N-terminal domain (280 amino acids). Tmn1 and Tmn2 exhibit the characteristic group II motif (FYLPGVAP and FSLPGLSP, respectively) and a long N-terminal domain (310 and 316 amino acids, respectively). Tmn3, like *Dictyostelium* Phg1c, does not exhibit characteristics of either group and cannot be classified unambiguously based on these criteria only.

Reconstruction of phylogenetic trees based on sequence similarities with human and *Dictyostelium* TM9 proteins led to the same conclusions (Fig. 1A): Tmn1 and Tmn2 are closely related to *Dictyostelium* Phg1a (group II); no *S. cerevisiae* TM9 protein could be unambiguously attributed to group I. In agreement

² The abbreviations used are: csA, contact site A; MAPK, mitogen-activated protein kinase.

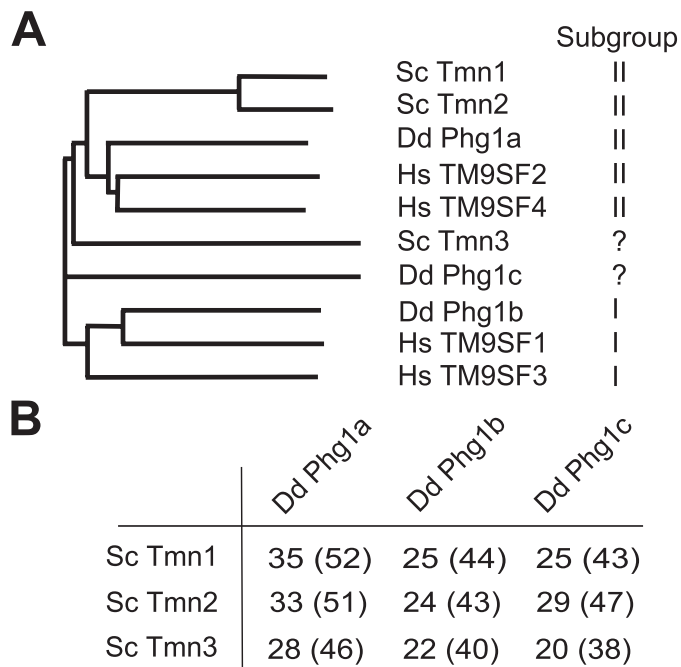


FIGURE 1. The TM9 family in *D. discoideum* and *S. cerevisiae*. *A*, phylogenetic tree of TM9 proteins in *D. discoideum* (Dd; Phg1a, b, c), human (Hs; TM9SF1, 2, 3, and 4), and *S. cerevisiae* (Sc; Tmn1, Tmn2, and Tmn3). The subgroup (I, II, or undetermined (?)) of each TM9 protein is indicated. *B*, degrees of identity and similarity (in parentheses) between TM9 proteins from *S. cerevisiae* and *D. discoideum*. Together these results suggest that yeast proteins Tmn1 and Tmn2 belong to the same subgroup as *D. discoideum* Phg1a.

with this, Tmn1 and Tmn2 exhibited the highest degree of identity with *Dictyostelium* Phg1a (Fig. 1B).

TM9 Proteins Are Essential for Yeast Cell Adhesion and Filamentous Growth—TM9 proteins play an essential role in *D. discoideum* cellular adhesion (2). Therefore, in budding yeast, we decided to first examine their role in adhesion. For this, we generated haploid and diploid yeast strains in the dimorphic Σ 1278b genetic background carrying deletions in the *TMN1*, *TMN2*, and *TMN3* genes in all possible combinations. The single, double, or triple deletion strains exhibited no obvious growth defect, suggesting that TM9 proteins are involved in a nonessential cellular function (data not shown). We also failed to detect differential growth in media containing various carbon sources including glucose, galactose, maltose, glycerol, and sucrose (data not shown). Finally, no effect of TM9 mutations on cell morphology or colony shape was apparent (data not shown).

In contrast, haploid strains lacking at least one of the three TM9 proteins were severely defective for adhesive growth (Fig. 2A). Single *tmn2* Δ and *Tmn1* Δ mutant strains retained a minimal capacity to adhere to the agar surface, whereas no adhesion was observed in the single *tmn3* Δ mutant or in any of the double and triple mutants. In diploid *S. cerevisiae* strains, cellular adhesion is required for the development of pseudohyphal filaments in response to nitrogen starvation (12, 23). Therefore, the requirement of TM9 proteins for filament formation was tested in homozygous diploid TM9 mutant strains grown on solid nitrogen starvation medium. We found that homozygous diploid single TM9 mutant strains had only a slightly reduced capacity to develop pseudohyphal filaments, whereas the dou-

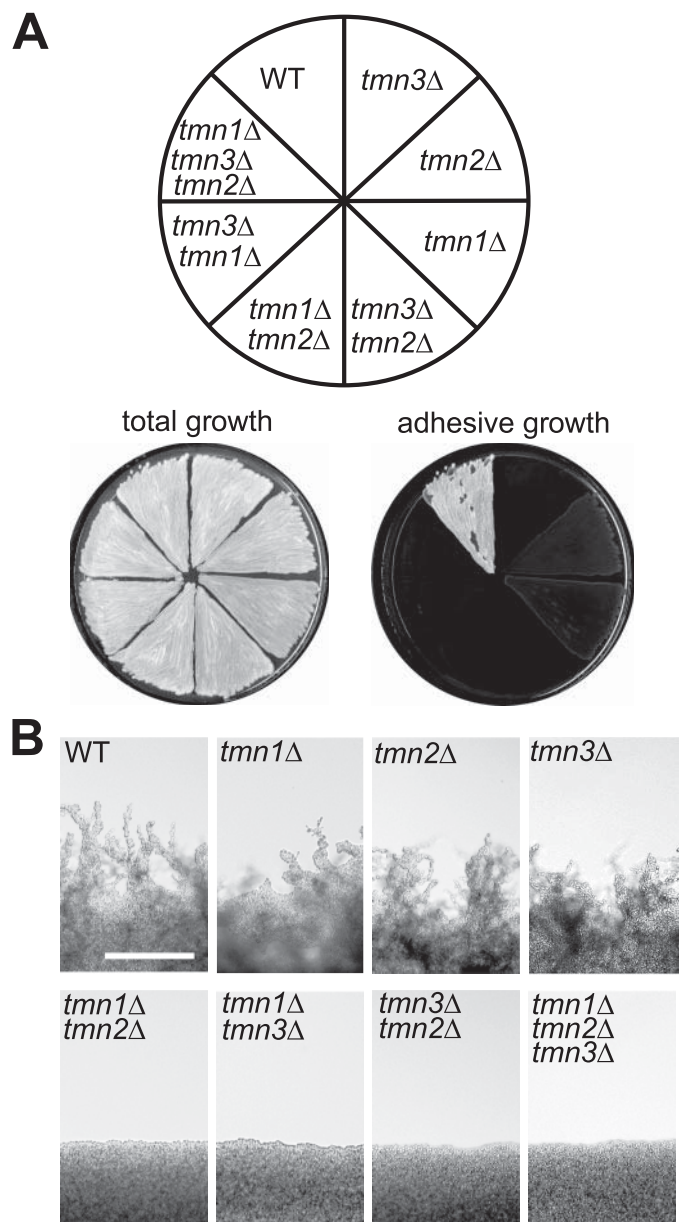


FIGURE 2. Role of TM9 proteins in cellular adhesion and filamentous growth in *S. cerevisiae*. *A*, adhesive growth is defective in TM9 mutant yeast. Haploid yeast strains of the indicated genotype were grown on solid YPD medium for 5 days at 30 °C, and the plates were photographed before (total growth) and after (adhesive growth) washing nonadhesive cells off the surface. *B*, filamentous growth of TM9 mutant cells. Diploid yeast strains of the indicated genotype were streaked on nitrogen starvation plates (synthetic low ammonia dextrose) to induce filamentous growth. The pictures were taken after 3 days of growth at 30 °C. Bar, 100 μ m.

ble and triple mutants were completely unable to grow in the filamentous form (Fig. 2B). Thus, although the mechanisms governing cellular adhesion in *S. cerevisiae* and in *D. discoideum* are very different, TM9 proteins also play an essential role in cellular adhesion and filamentous growth in the budding yeast *S. cerevisiae*.

TM9 Proteins Are Required for Expression of *FLO11* and Act Downstream of *Ras2* and *TOR*—The morphogenetic switch to filamentous growth in *S. cerevisiae* involves the cooperation of at least two different signaling pathways, a MAPK cascade and a cAMP-dependent pathway (16, 24–27) (Fig. 3A). A central

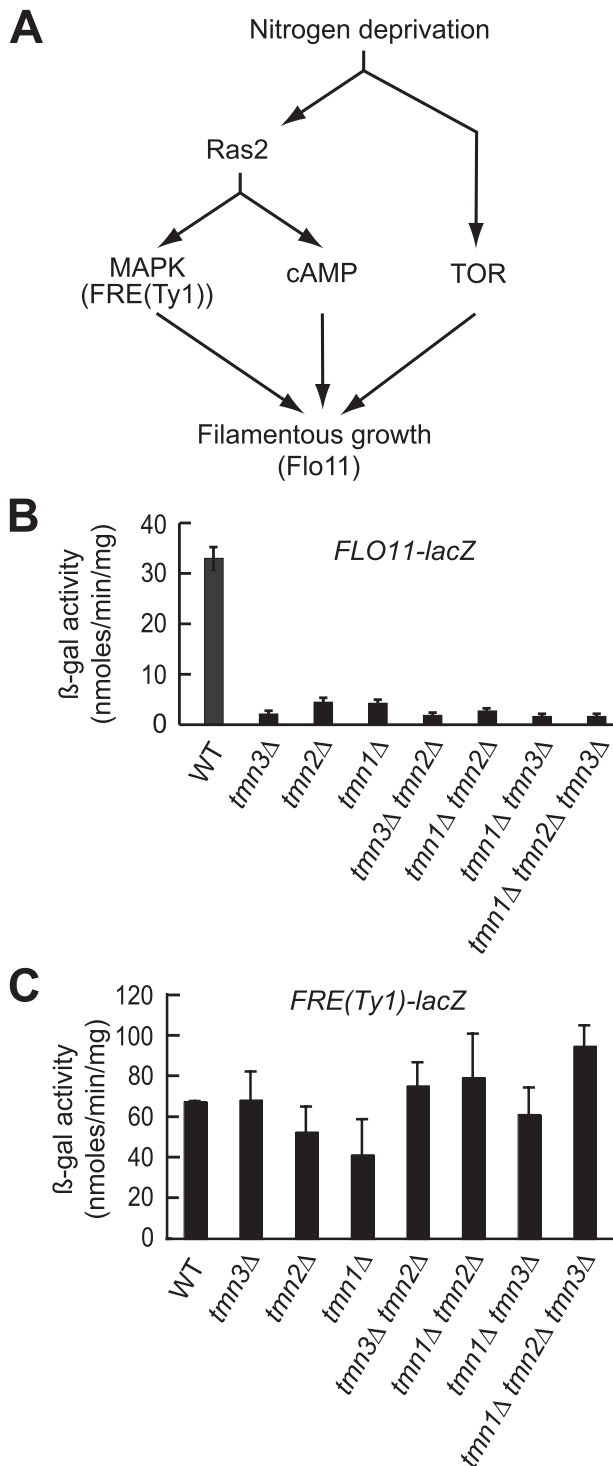


FIGURE 3. Effect of TM9 mutations on gene expression. A, the morphogenetic switch to filamentous growth in *S. cerevisiae* involves the cooperation of different signaling pathways. A MAPK cascade and a cAMP-dependent pathway are controlled by the GTP-binding protein Ras2. The TOR pathway also participates in the physiological response to starvation independently of the MAPK or cAMP pathways. These pathways converge to regulate the expression of the *FLO11* gene, which encodes a cell surface flocculin. B, role of TM9 proteins in *FLO11-lacZ* expression. Haploid yeast strains of the indicated genotype carrying plasmid B3782 (*FLO11-lacZ*) were assessed for β -galactosidase activity during growth in logarithmic phase in liquid YNB medium. The β -galactosidase activity is expressed in nmol/min/mg of cellular proteins. The bars depict the mean values \pm standard deviations of three transformants, each determined in triplicate. C, expression of *FRE(Ty1)::LacZ* reporter gene in TM9 mutant strains. β -Galactosidase activity was measured in diploid strains carrying the plasmid pFRE(Ty1)::LacZ during growth in logarithmic phase in liquid YNB medium.

element of these two pathways is the GTP-binding protein Ras2, which is thought to stimulate the transcription factor Ste12 via the MAPK pathway. In the cAMP-dependent pathway, activated Ras2 can interact with adenylate cyclase, and this results in an increase of cAMP, which in turn activates cAMP-dependent protein kinases and leads to the activation of Flo8. The TOR pathway also plays a role in sensing nitrogen sources and regulating physiological responses independently of the MAPK and cAMP pathways (28). These pathways converge to regulate the expression of the *FLO11* gene, which encodes a cell surface flocculin (Fig. 3A), which mediates cell adhesion (29, 30). Numerous studies have shown specifically that in the dimorphic $\Sigma 1278b$ genetic background, expression of the cell surface flocculin Flo11 is essential for adhesive growth and filament formation (16, 31, 32). We therefore tested whether expression of *FLO11* might be affected by mutations in TM9 genes. We found that in all haploid TM9 mutant strains, expression of a *FLO11-lacZ* reporter gene was strongly reduced when compared with a wild-type strain (Fig. 3B). Similar results were obtained with diploid strains (data not shown). Thus, TM9 proteins appear to be involved in the regulation of the expression of adhesion molecules in yeast.

To further explore the role of TM9 proteins in regulation of cellular adhesion, we performed a genetic epistasis analysis by expressing the dominant active *RAS2^{VAL19}* allele. As expected, this led to increased filament formation in the control strains, but this effect was completely inhibited in all TM9 double and the triple mutant strains (data not shown). Similarly, TOR1 overexpression did not restore filamentous growth in double or triple TM9 mutants (data not shown). These results indicate that TM9 proteins act downstream of the Ras/cAMP and TOR pathways to control *FLO11* expression.

The activity of the MAPK pathway can be monitored by the *FRE(Ty1)-lacZ* reporter gene, the expression of which depends on elements of the Kss1-MAPK cascade and the combined action of the transcription factors Ste12 and Tec1 (15, 17). Here, we found that expression of *FRE(Ty1)-lacZ* was not reduced in TM9 mutant strains (Fig. 3C), indicating that TM9 proteins do not affect *FLO11* gene expression and filamentous growth by inhibiting the Kss1-MAPK pathway.

Taken together, these results suggest that in the budding yeast, TM9 proteins play a critical role in the late stages of a nutrient-controlled pathway notably regulating *FLO11* gene expression. These observations prompted us to investigate the possibility of a link between TM9 proteins and nutrient-controlled functions in *Dictyostelium*.

Dictyostelium Phg1 Proteins Are Not Implicated in Initiation of Development or of Autophagy—In *Dictyostelium*, multicellular development, autophagy, and secretion of lysosomal enzymes are all critically controlled by nutrient availability. To test the potential involvement of TM9 proteins in these functions in *D. discoideum*, we made use of TM9 mutant cells (named *phg1* or *phg1a* and *phg1b* in *D. discoideum*) described previously (3) and assessed nutrient-controlled functions in wild-type and mutant cells. Specifically, we examined the phenotypes of *phg1a*, *phg1b*, and the double *phg1a/b* mutant cells. In addition, we analyzed *phg1a* mutant cells overexpressing Phg1b (*phg1a+PHG1b*). To monitor the initiation of develop-

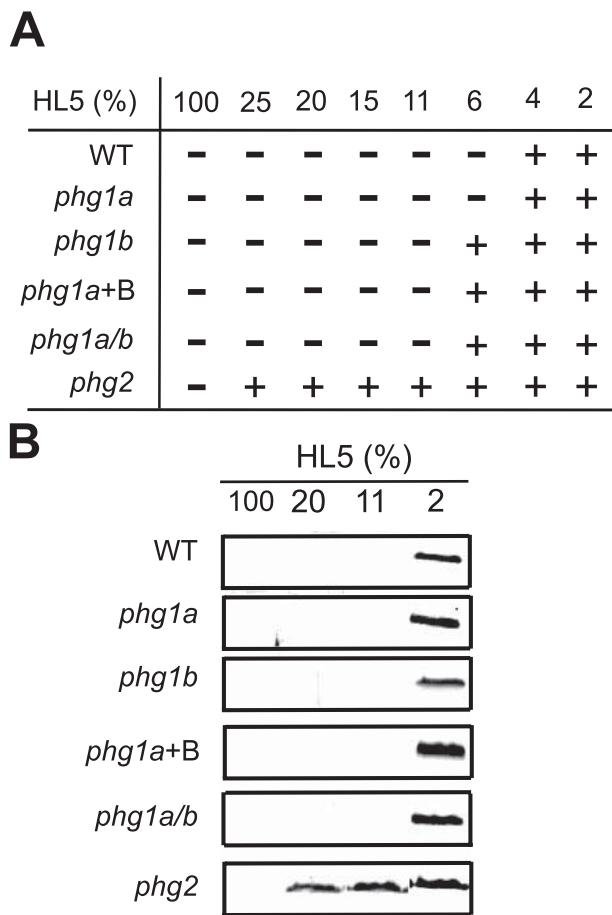


FIGURE 4. Initiation of multicellular development is normal in *phg1a* mutant cells. A, wild-type and mutant cells were placed for 24 h in a medium containing a defined amount of nutrients, obtained by diluting HL5 medium with phosphate buffer. After 24 h, multicellular development was monitored by assessing the presence (+) or absence (–) of tight cellular aggregates. Unlike wild-type and *phg1* cells, *phg2* mutant cells initiated multicellular development at high concentrations of nutrients. B, cells treated as in A were harvested, and the expression of *csA* was determined by Western blot analysis.

ment, we incubated wild-type or mutant cells in medium containing a defined amount of nutrients and followed the formation of multicellular aggregates. This test has proven useful to demonstrate abnormalities in the initiation of multicellular development, as observed for example in cells defective in the *Phg2* kinase (20). In wild-type or in *phg1* mutant cells, the induction of multicellular aggregates was inhibited by a low concentration of nutrients (4–6% HL5 medium) (Fig. 4A). This was further confirmed by determining the expression of *csA*, a well characterized marker of multicellular development (Fig. 4B).

Nutrient starvation also induces the expression of a collection of genes involved in autophagy in *Dictyostelium* (33–36). To detect an abnormal autophagy induction by nutrients, we measured by real time PCR the expression of three autophagy genes, *ATG1*, *ATG8*, and *ATG9*, in wild-type, *phg2*, and various *phg1* mutant cells. The expression of these marker genes was not induced in HL5 medium in wild-type or mutant cells (Fig. 5 and supplemental Fig. S1). Thus, autophagy appears normally inhibited by nutrients in all *phg1* mutant cells as well as in *phg2* mutant cells. Starvation induced the expression of autophagy

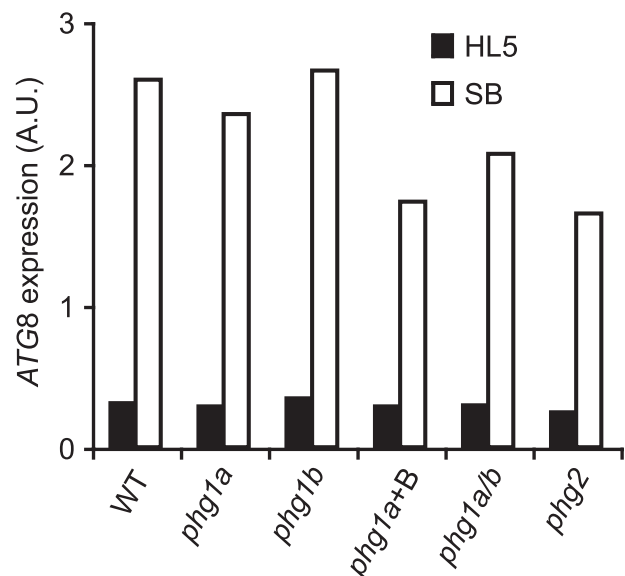


FIGURE 5. *Phg1* mutant cells induce normal transcription of the *ATG8* autophagy gene. Wild-type and mutant cells were grown in HL5 medium for 3 days to a final density of 10^6 cells/ml. The cells were then harvested, and RNA samples were extracted. Expression of *ATG8* was quantified by real time PCR. Alternatively, the cells were starved in phosphate buffer (SB) for 6 h to induce expression of *ATG8*. Similar results were obtained when the expression of *ATG1* and *ATG9* was assessed (supplemental Fig. S1).

genes in wild-type and in *phg1* mutant cells (Fig. 5 and supplemental Fig. S1), confirming that *Phg1* proteins are not involved in the induction of autophagy in *Dictyostelium*.

Secretion of Lysosomal Enzymes Is Dysregulated in *Dictyostelium* TM9 Mutant Cells—The third phenomenon controlled by nutrients in *Dictyostelium* is the regulated secretion of lysosomal enzymes. Lysosomal enzymes are normally synthesized in the ER and transported to lysosomal compartments where they are activated by limited proteolysis (37). Upon starvation, the cells secrete defined amounts of each lysosomal enzyme, for example a large percentage of *N*-acetyl β -glucosaminidase or α -mannosidase, and a more moderate fraction of the acid phosphatase pool (38). *N*-Acetyl β -glucosaminidase, α -mannosidase, and acid phosphatase activities were measured in cells and in the medium after 3 days of cellular growth in HL5 medium. Interestingly, in yeast, synthetic lethality has been observed between TM9 genes and YPT6 (39). Because YPT6 is involved in the function of the endocytic pathway, this suggests a link between TM9 proteins and the endocytic pathway. Wild-type cells and *phg2* mutant cells secreted ~10% of their total lysosomal enzymes in HL5 medium. In contrast, *phg1a* mutant cells secreted a huge amount of hydrolases: 85% of *N*-acetyl β -glucosaminidase and α -mannosidase and 30% of the acid phosphatase pool were found in the extracellular medium (Fig. 6A and supplemental Table S1). This secretion was continuous and observed even immediately after cells were transferred to fresh HL5 medium (Fig. 6B), demonstrating that secretion of lysosomal enzymes in *phg1a* mutant cells was not inhibited by nutrients. A similar phenotype was also observed in *phg1a/b* double knock-out cells (Fig. 6). Interestingly, *phg1b* mutant cells also secreted abnormally lysosomal enzymes, albeit not as much as *phg1a* (Fig. 6). Moreover, overexpression of *Phg1b* in *phg1a* mutant cells caused a marked decrease of enzyme secretion

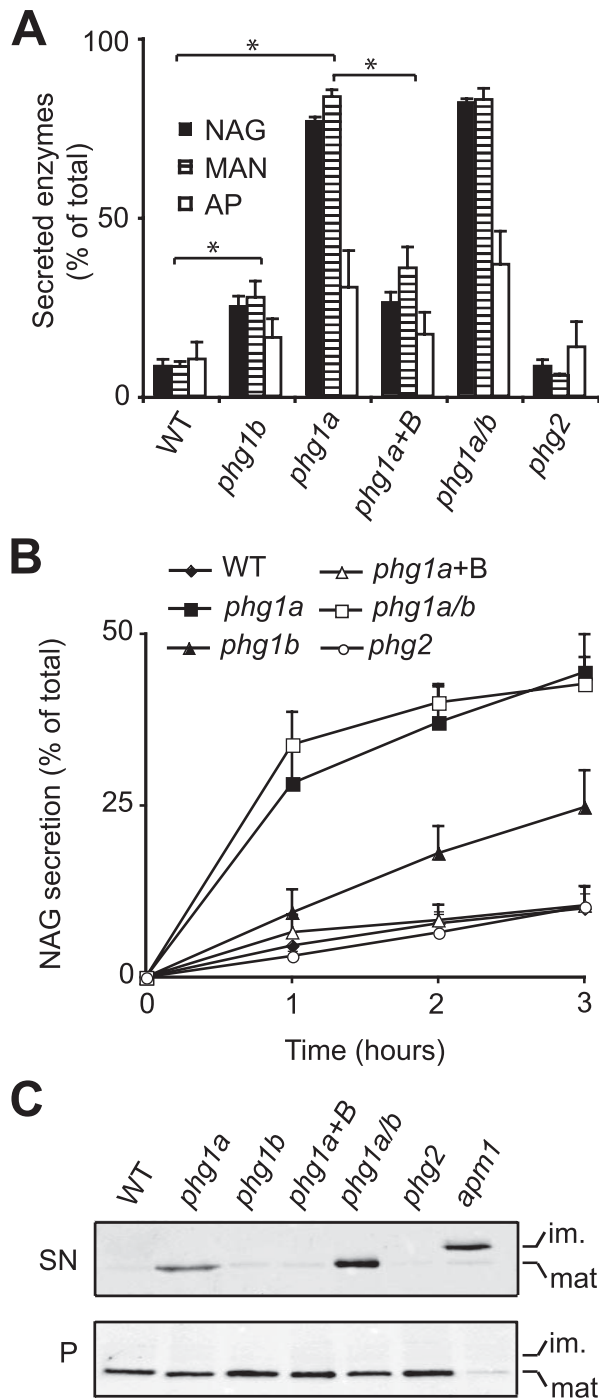


FIGURE 6. Phg1 mutant cells secrete mature lysosomal enzymes in rich medium. A, wild-type or mutant cells were grown in HL5 medium for 3 days to a final density of 2×10^6 cells/ml. The cells were harvested and centrifuged, and the activity of lysosomal enzymes was determined in cell pellets and in supernatants. The fraction of enzymatic activity found in the supernatant is indicated. The total amount of enzymatic activity (secreted + intracellular) was similar in all strains analyzed (supplemental Table S1). NAG, N-acetyl β -glucosaminidase; MAN, α -mannosidase; AP, acid phosphatase. The results presented are the averages and S.E. of three independent experiments. *, $p < 0.01$ (Student's t test). B, wild-type or mutant cells were collected and incubated in fresh HL5 medium. After 0, 1, 2, and 3 h, the NAG activity was determined and expressed as described above. C, cells were grown and processed as described in A. Procatepsin D (im., 53 kDa) and cathepsin D (mat., 44 kDa) were detected by Western blot in the cell pellet (P) and in the medium (SN). In wild-type and *phg2* cells, mature cathepsin was retained in the cells. In *phg1a* and in *phg1a/phg1b* mutant cells, mature cathepsin D was secreted in the extracellular medium. For comparison, *apm1* mutant cells in which targeting to the lysosomes is defective secreted immature procatepsin D.

(Fig. 6). As expected, starved wild-type and mutant cells all secreted efficiently lysosomal enzymes in the medium (supplemental Fig. S2).

Lysosomal enzymes could conceivably be secreted either directly after their passage through the Golgi apparatus or after their targeting to lysosomal compartments. To distinguish between these two possibilities, procathepsin D and cathepsin D were detected by Western blot in cell pellets and supernatants. *Phg1a* mutant cells secreted cathepsin D in its mature form, whereas, as described previously (9), *apm1* mutant cells secreted the precursor form (Fig. 6C). This defect was also complemented by overexpression of Phg1b. As expected, the double knock-out *phg1a/phg1b* cells secreted also a mature form of cathepsin D (Fig. 6C). Together, these results demonstrate that the dysregulated secretion of lysosomal enzymes by *phg1a* mutant cells is not caused by a defect in targeting to the lysosomes but rather by a defect in the regulation of lysosomal enzyme secretion. They also indicate a certain degree of redundancy between Phg1a and Phg1b for the control of lysosomal enzyme secretion in *Dictyostelium*, as evidenced by the partial complementation of the phenotype of *phg1a* mutant cells by the overexpression of Phg1b.

Besides defects in lysosome enzyme secretion, we detected no general defect in the morphology of endocytic compartments labeled with antibodies against the p80 endosomal marker and the vacuolar H^+ -ATPase (40) (data not shown). Endocytosis of a fluid phase marker, as well as its subsequent recycling to the extracellular medium were also tested. Fluid phase was endocytosed in wild-type and in mutant cells at the same rate (Fig. 7A and supplemental Fig. S3). After loading cells for 2 h in HL5 containing Alexa 647-coupled dextran, recycling was measured. Internalized fluorescence was released in the medium with similar kinetics in wild-type and *phg1* mutant cells (Fig. 7B and supplemental Fig. S3). These results indicate that the overall organization and function of the endocytic pathway are not grossly altered in *phg1a* mutant cells.

DISCUSSION

The presence of nutrients is a major regulator of eucaryotic cell physiology. Starvation induces autophagy in many very different cellular systems ranging from mammalian cells to amoebae or yeast. In addition, it can induce more specific responses in different systems, for example invasive growth in yeast and in *Dictyostelium* regulated secretion of lysosomal enzymes and multicellular development. Our results indicate that in yeast and in *Dictyostelium*, a subset of these specific responses implicates TM9 proteins. Indeed, in both organisms, some nutrient-controlled responses are still normal in TM9 mutant cells (e.g. induction of the MAPK pathway by starvation in yeast or induction of autophagy and multicellular development in starved *Dictyostelium*). This indicates that these cells are still able to sense the presence or absence of nutrients. However some specific responses to nutrients are affected in TM9 mutant cells, notably filamentous growth in yeast and lysosomal enzyme secretion in *Dictyostelium*. Our results in yeast further suggest that TM9 proteins are critical at a late stage of signal transduction, because upstream elements of the nutrient-sensing pathways (MAPK pathway) are still functional in TM9 mutants,

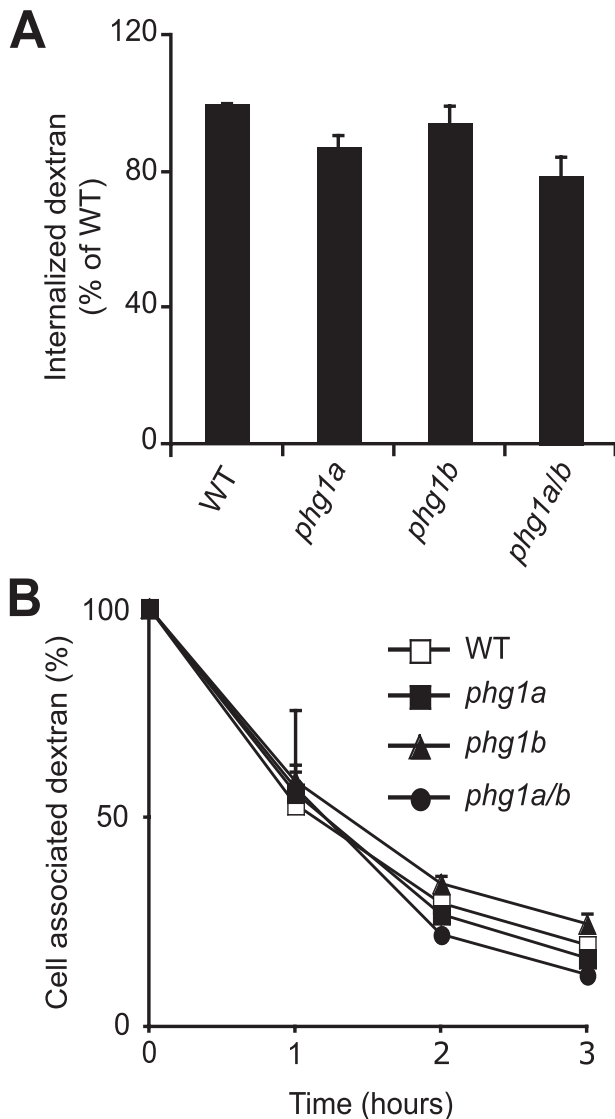


FIGURE 7. Fluid phase uptake and recycling are not altered in *phg1* mutant cells. *A*, wild-type and mutant cells were incubated for 1 h in HL5 medium containing 10 μ g/ml of fluorescent dextran. Internalized fluorescence was measured by flow cytometry. *B*, cells were incubated in HL5 containing fluorescent dextran for 2 h, then washed, and transferred to fresh HL5 medium for the indicated time. Internal fluorescence was measured at each time point and expressed as a percentage of the signal at time 0. Recycling of fluid phase to the extracellular medium was similar in wild-type and mutant cells. Similar results were obtained for *phg1a* cells overexpressing Phg1b and for *phg2* mutant cells (supplemental Fig. S3).

whereas late stages (induction of FLO11) are defective. The most simple interpretation of these observations is that a TM9-controlled signaling pathway converges with nutrient-sensing pathways at a late stage and controls specifically a few elements of cellular physiology. According to this model, the detailed organization of the nutrient-sensing and TM9 signaling pathways in various organisms would account for the fact that synergistic or antagonistic relationships can be observed in different situations. Interestingly, in this study, we observed clear functional redundancy between TM9 proteins in yeast, as well as in *Dictyostelium*. This is compatible with the notion that all TM9 proteins act in at least partially overlapping signaling pathways. However, although functional redundancy can often account for wild-type phenotypes in single knock-out mutants,

this was not the case for single TM9 mutants, which exhibited clear phenotypes in yeast as well as in *Dictyostelium*. This suggests that TM9 proteins participate in a very finely tuned signaling network controlling a few critical elements of cellular physiology. More detailed studies will be necessary to determine the exact role played by TM9 proteins in cellular signal transduction pathways.

Because this study was performed in parallel in two very different organisms, it is interesting to compare the elements of the cellular physiology that are placed specifically under the control of TM9 proteins in these two situations. In yeast, filamentous growth requires the expression of specific adhesion molecules and polarized budding. It is believed to represent a coordinated program allowing invasive growth. In conditions of nutrient depletion, yeast cells can thus invade their substrate, and this can allow them to uncover new sources of nutrients. When switched to a medium containing no nutrients, *Dictyostelium* amoebae also undergo a series of successive changes. Within minutes, they start secreting lysosomal enzymes (38). Over a longer period of time (a few hours), they express proteins necessary for autophagy, probably to obtain amino acids by digesting cytosolic proteins. Finally, upon prolonged starvation (>6 h), expression of appropriate genes allows the initiation of multicellular development. Remarkably, only the first part of this response (secretion of lysosomal enzymes) is affected in TM9 mutant cells; unlike wild-type cells, these mutant cells secrete mature lysosomal enzymes even in the presence of nutrients, suggesting that the dysregulated secretion of lysosomal enzymes is not caused by a defect in targeting to lysosomes but rather by an abnormal regulation of lysosome secretion. In addition to this phenotype, previous studies have shown that adhesion of TM9 mutant cells to their substrates is modified; cells retain only the ability to adhere to certain substrates, possibly reflecting a change in their surface adhesion molecules (2, 3). We speculate here that the TM9-controlled response in *Dictyostelium* represents an invasive growth program similar to that described in yeast. Indeed, changes in cell adhesion and secretion of lysosomal enzymes should allow starved *Dictyostelium* cells to digest and invade their substrate and possibly to uncover new sources of nutrients. If this hypothesis is true, we should expect future studies to reveal more common elements between the control of invasive growth in budding yeast and in *Dictyostelium* amoebae.

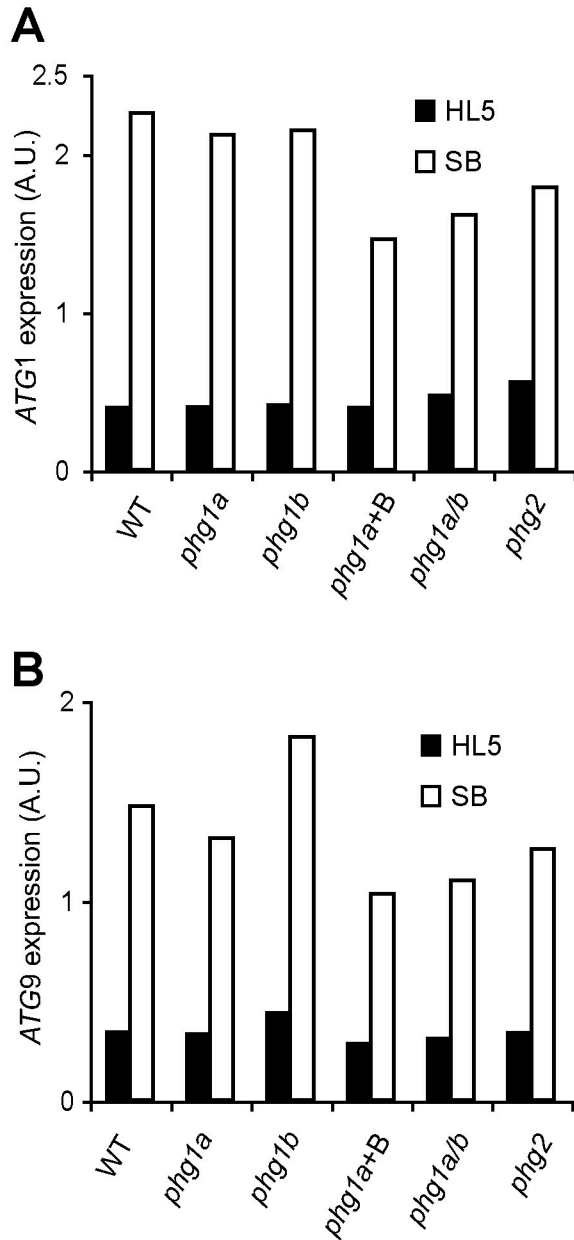
Acknowledgments—We thank Dr. Valeria Wanke, Dr. Mylène Docquier, and Didier Chollet for technical assistance.

REFERENCES

1. Chluba-de Tapia, J., de Tapia, M., Jaggin, V., and Eberle, A. N. (1997) *Gene (Amst.)* **197**, 195–204
2. Benghezal, M., Cornillon, S., Gebbie, L., Alibaud, L., Bruckert, F., Letourneur, F., and Cosson, P. (2003) *Mol. Biol. Cell* **14**, 2890–2899
3. Cornillon, S., Pech, E., Benghezal, M., Ravanel, K., Gaynor, E., Letourneur, F., Bruckert, F., and Cosson, P. (2000) *J. Biol. Chem.* **275**, 34287–34292
4. Schiestl, R. H., and Petes, T. D. (1991) *Proc. Natl. Acad. Sci. U. S. A.* **88**, 7585–7589
5. Wach, A., Brachat, A., Pohlmann, R., and Philippsen, P. (1994) *Yeast* **10**, 1793–1808
6. Lorenz, M. C., Muir, R. S., Lim, E., McElver, J., Weber, S. C., and Heitman, J.

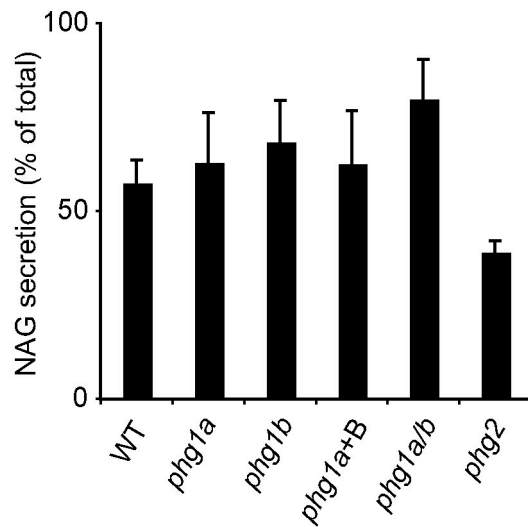
- J. (1995) *Gene (Amst.)* **158**, 113–117
7. Caterina, M. J., Milne, J. L., and Devreotes, P. N. (1994) *J. Biol. Chem.* **269**, 1523–1532
8. Gebbie, L., Benghezal, M., Cornillon, S., Froquet, R., Cherix, N., Malbouyres, M., Lefkir, Y., Grangeasse, C., Fache, S., Dalous, J., Bruckert, F., Letourneur, F., and Cosson, P. (2004) *Mol. Biol. Cell* **15**, 3915–3925
9. Lefkir, Y., de Chassey, B., Dubois, A., Bogdanovic, A., Brady, R. J., Destaing, O., Bruckert, F., O'Halloran, T. J., Cosson, P., and Letourneur, F. (2003) *Mol. Biol. Cell* **14**, 1835–1851
10. Journet, A., Chapel, A., Jehan, S., Adessi, C., Freeze, H., Klein, G., and Garin, J. (1999) *J. Cell Sci.* **112**, 3833–3843
11. Bertholdt, G., Stadler, J., Bozzaro, S., Fichtner, B., and Gerisch, G. (1985) *Cell Differ.* **16**, 187–202
12. Gimeno, C. J., Ljungdahl, P. O., Styles, C. A., and Fink, G. R. (1992) *Cell* **68**, 1077–1090
13. Broek, D., Toda, T., Michaeli, T., Levin, L., Birchmeier, C., Zoller, M., Powers, S., and Wigler, M. (1987) *Cell* **48**, 789–799
14. Helliwell, S. B., Wagner, P., Kunz, J., Deuter-Reinhard, M., Henriquez, R., and Hall, M. N. (1994) *Mol. Biol. Cell* **5**, 105–118
15. Mosch, H. U., Roberts, R. L., and Fink, G. R. (1996) *Proc. Natl. Acad. Sci. U. S. A.* **93**, 5352–5356
16. Rupp, S., Summers, E., Lo, H. J., Madhani, H., and Fink, G. (1999) *EMBO J.* **18**, 1257–1269
17. Madhani, H. D., and Fink, G. R. (1997) *Science* **275**, 1314–1317
18. Rose, M., and Botstein, D. (1983) *Methods Enzymol.* **101**, 167–180
19. Dimond, R. L., Knecht, D. A., Jordan, K. B., Burns, R. A., and Livi, G. P. (1983) *Methods Enzymol.* **96**, 815–828
20. Cherix, N., Froquet, R., Charette, S. J., Blanc, C., Letourneur, F., and Cosson, P. (2006) *Mol. Biol. Cell* **17**, 4982–4987
21. Singer-Kruger, B., Frank, R., Crausaz, F., and Riezman, H. (1993) *J. Biol. Chem.* **268**, 14376–14386
22. Sugawara, T., Lenzen, G., Simon, S., Hidaka, J., Cahen, A., Guillaume, J. L., Camoin, L., Strosberg, A. D., and Nahmias, C. (2001) *Gene (Amst.)* **273**, 227–237
23. Mosch, H. U., and Fink, G. R. (1997) *Genetics* **145**, 671–684
24. Gancedo, J. M. (2001) *FEMS Microbiol. Rev.* **25**, 107–123
25. Pan, X., Harashima, T., and Heitman, J. (2000) *Curr. Opin. Microbiol.* **3**, 567–572
26. Liu, H., Styles, C. A., and Fink, G. R. (1993) *Science* **262**, 1741–1744
27. Roberts, R. L., and Fink, G. R. (1994) *Genes Dev.* **8**, 2974–2985
28. Cutler, N. S., Pan, X., Heitman, J., and Cardenas, M. E. (2001) *Mol. Biol. Cell* **12**, 4103–4113
29. Guo, B., Styles, C. A., Feng, Q., and Fink, G. R. (2000) *Proc. Natl. Acad. Sci. U. S. A.* **97**, 12158–12163
30. Verstrepen, K. J., and Klis, F. M. (2006) *Mol. Microbiol.* **60**, 5–15
31. Lo, W. S., and Dranginis, A. M. (1998) *Mol. Biol. Cell* **9**, 161–171
32. Braus, G. H., Grundmann, O., Bruckner, S., and Mosch, H. U. (2003) *Mol. Biol. Cell* **14**, 4272–4284
33. Otto, G. P., Wu, M. Y., Kazgan, N., Anderson, O. R., and Kessin, R. H. (2004) *J. Biol. Chem.* **279**, 15621–15629
34. Otto, G. P., Wu, M. Y., Kazgan, N., Anderson, O. R., and Kessin, R. H. (2003) *J. Biol. Chem.* **278**, 17636–17645
35. Otto, G. P., Wu, M. Y., Clarke, M., Lu, H., Anderson, O. R., Hilbi, H., Shuman, H. A., and Kessin, R. H. (2004) *Mol. Microbiol.* **51**, 63–72
36. Kosta, A., Roisin-Bouffay, C., Luciani, M. F., Otto, G. P., Kessin, R. H., and Golstein, P. (2004) *J. Biol. Chem.* **279**, 48404–48409
37. Richardson, J. M., Woychik, N. A., Ebert, D. L., Dimond, R. L., and Cardelli, J. A. (1988) *J. Cell Biol.* **107**, 2097–2107
38. Dimond, R. L., Burns, R. A., and Jordan, K. B. (1981) *J. Biol. Chem.* **256**, 6565–6572
39. Tong, A. H., Lesage, G., Bader, G. D., Ding, H., Xu, H., Xin, X., Young, J., Berriz, G. F., Brost, R. L., Chang, M., Chen, Y., Cheng, X., Chua, G., Friesen, H., Goldberg, D. S., Haynes, J., Humphries, C., He, G., Hussein, S., Ke, L., Krogan, N., Li, Z., Levinson, J. N., Lu, H., Menard, P., Munyana, C., Parsons, A. B., Ryan, O., Tonikian, R., Roberts, T., Sdicu, A. M., Shapiro, J., Sheikh, B., Suter, B., Wong, S. L., Zhang, L. V., Zhu, H., Burd, C. G., Munro, S., Sander, C., Rine, J., Greenblatt, J., Peter, M., Bretscher, A., Bell, G., Roth, F. P., Brown, G. W., Andrews, B., Bussey, H., and Boone, C. (2004) *Science* **303**, 808–813
40. Ravel, K., de Chassey, B., Cornillon, S., Benghezal, M., Zulianello, L., Gebbie, L., Letourneur, F., and Cosson, P. (2001) *Eur. J. Cell Biol.* **80**, 754–764
41. Sikorski, R. S., and Hieter, P. (1989) *Genetics* **122**, 19–27

Figure S1



Supplemental fig. S1. Transcription of *ATG1* and *ATG9* is unaffected in *phg1* mutant cells. Wild-type and mutant cells were incubated in HL5 or SB, and the expression of *ATG1* (A) and *ATG9* (B) assessed as described in the Legend to Fig. 5. *Phg1* mutant cells did not exhibit anomalies in the induction of autophagy genes.

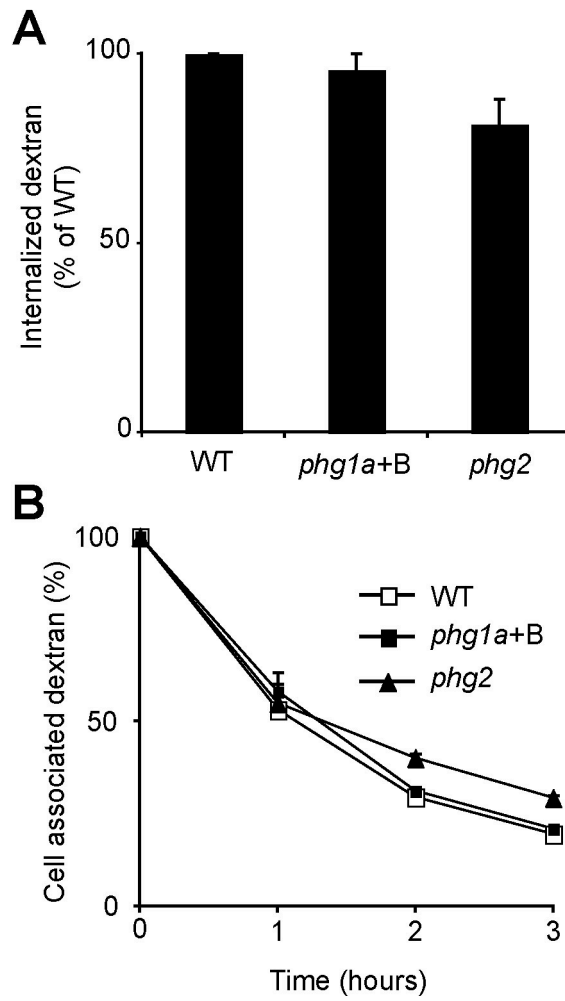
Figure S2



Supplemental fig S2. Starved *phg1* mutant cells secrete lysosomal enzymes.

Wild-type or mutant cells were incubated for 6 hours in phosphate buffer to induce lysosomal enzyme secretion. Results are expressed as the percentage of total enzymatic activity detected in the extracellular medium.

Figure S3



Supplemental fig. S3. Fluid phase uptake and recycling are not altered in *phg1* mutant cells. Fluid phase uptake (A) and recycling (B) were measured as described in the Legend to figure 7.

	WT	<i>phg1a</i>	<i>phg1b</i>	<i>phg1a+B</i>	<i>phg1a/b</i>	<i>phg2</i>
NAG	845+/-129	601+/-173	848+/-198	941+/-313	432+/-54	1132+/-24
MAN	173+/-22	198+/-28	175+/-25	230+/-58	147+/-31	271+/-41
AP	54+/-7	79+/-16	58+/-14	88+/-24	76+/-3	56+/-6

Table S1. Total lysosomal enzymatic activity in wild-type and mutant cells (cell-associated+secreted). The mean and SEM of three independent experiments are indicated. In these three experiments, analyzed further in Fig. 6A, the total amount of lysosomal enzymes did not vary significantly.